16th World Conference on Earthquake, 16WCEE 2017

Santiago Chile, January 9th to 13th 2017

Paper N° 1021

Registration Code: S-S1461664114

NUMERICAL STUDY ON BRIDGE ELASTOMERIC BEARINGS SUBJECTED TO LARGE SHEAR STRAINS WITH EMPHASIS ON LOCAL TENSION

K. N. Kalfas[(1)], S. A. Mitoulis[(2)], K. Katakalos[(3)]

[(1)] *Site Engineer, COSTAIN Engineering & Construction Limited, kostas.kalfas@costain.com*
[(2)] *Assistant Professor, University of Surrey, s.mitoulis@surrey.ac.uk, www.mitoulis.com*
[(3)] *Research Associate, Aristotle University of Thessaloniki, kkatakal@civil.auth.gr*

Abstract

Steel-laminated elastomeric bearings are common structural components used in isolated structures. Elastomeric bearings are proven to be excellent isolators of vibrations for bridges, as they shift the fundamental period of the structure and increase the damping, hence mitigate seismic effects. However, recent failures of isolators in South America and Asia (the 2010 Chile Earthquake in Chile, the 2011 Great Tohoku earthquake in Japan) have shown that the methods for the design of elastomeric bearings require improvements. Under seismic excitations, global and local tensile stresses might be developed within the elastomer of bearings, causing fluctuations of their vertical load. An overall study of the international literature proved an acknowledged gap regarding the response of elastomeric bearings under variable axial loads. This paper investigates the response of steel-laminated elastomeric bearings through extensive numerical modelling calibrated against published numerical and experimental results. Analyses with cyclic shear displacements and variable axial loads were performed to better understand their response, i.e. their damping and stiffness at large strains and also the development of local tensile stresses. The hyperelastic Ogden model is used to simulate the mechanical properties of the elastomeric material of the bearing. The study identified the response of steel-laminated elastomeric bearings and the development of local tensile stresses under multiple cycles of loading - unloading, variable combined loads and different boundary conditions. Experimental tests are being conducted at the University of Surrey, in order for the results of this paper to be validated.

Keywords: bridge isolation; steel-laminated elastomeric bearings; damping; stiffness; local tension

1. Introduction

Elastomeric bearings are used widely in base isolation schemes for mitigating the dynamic loads on bridges [1-4]. They accommodate movements – horizontal, vertical and rotations - that are developed in bridges, due to thermal effects and seismic excitations [5-6]. More specifically, bearings accommodate seismic movements and increase the fundamental period of the structure hence the structure is away from the dominant periods of the seismic motions. Widely used in civil, mechanical and automotive engineering since the early 1980s, multilayer rubber bearings have been used as seismic isolation devices for buildings in highly seismic areas in many countries. Nonetheless, the multilayer rubber bearings are not the only devices which are used as anti-seismic devices. Such devices, which provide isolation to the structures, are the viscous dampers (by improving efficient energy dissipation) or the Shock Transmitted Units (STU, which provide additional dynamic restraints). Their appeal in these applications comes from their ability to provide a component with high stiffness in the vertical direction and high flexibility in the two horizontal directions. This combination of vertical stiffness with horizontal flexibility, achieved by reinforcing the rubber by thin steel shims perpendicular to the vertical load [7]. With regard to international literature, emphasis was placed on the shear and compressive response of the isolators under design basis earthquakes by performing numerical tests and experiments [8-10]. On the contrary little emphasis was placed on the tensile response of the isolators [5, 12-13]. The potential of tensile stresses within bridge bearings exists and depends on the shape factor of the isolators [6, 11]. Nonetheless, the tensile stresses that are developed within the elastomer were initially investigated by Gent and Lindley [14]. Their study observed that the strength of the rubber was subjected to severe degradation when 2.75 MPa of tensile stress was imposed to the elastomer.

The role of steel-laminated elastomeric bearings, when used as base isolation system in order to isolate the bridge deck, is to sustain the transmission of the compressive loads due to the self-weight of the deck. However, reconnaissance surveys, following major earthquakes in South America and Asia (the 2010 Chile Earthquake, the 2011 off the Pacific coast of Tohoku earthquake in Japan) [15-16], revealed that the bearings might be subjected to tensile stresses, even when the global response of the isolator is shearing and axial compression. The studies by Kawashima and Matsuzaki [17] and Kawashima et al. [18] revealed that damages on the bridges occurred due to the subsequent tsunami waves, instead of the earthquake itself. The Japanese bridges which had been designed by post-1990 Codes incorporated elastomeric bearings and the existing unseating prevention devices had been enhanced [17-18]. Nonetheless, quite a few bridges did not avoid the extensive damage [17]. In the 2010 Chile Earthquake was remarked one of the most prevalent failure modes of bridges after seismic actions, the unseating of the decks [15], an event which causes rupture of elastomeric bearings.

Nowadays there are different codes and standards available which cover the design of bearings. The complexity of the stresses and their development within the isolators has led to different requirements between these codes and standards. According to EN 1337-3 [19], the bearing is exposed to the possibility of tensile loading. For such tensile stresses, restrainers or unseating prevention devices can be used. BS EN 15129 [20] and EN 1337-3 [19] allow the development of tensile stresses within elastomer of bearings up to $2G$, where G is the shear modulus of the elastomer, and its value ranges between 0.55 MPa and 1.2 MPa. On the other hand, based on AASHTO [21], tensile stresses up to $2\text{-}3G$ might be developed within the bearing, hence the limit value of tensile stresses, that AASHTO [21] sets, is in the range of 2 to 3 MPa, assuming a typical value of G of 1 MPa. Similarly, the JRA [22] allows small tensile stresses within the elastomeric bearings, up to 2 MPa. In aseismic design code of China, the tensile stress is limited to 1 MPa [23]. Also, there should be no uplift of the isolators under seismic excitations according to Eurocode 8-Part 2 [24]. Based on the aforementioned codes, it is evident that the tensile response of bearings is a matter that has different design approaches, as can be seen in Fig. 1, and requires further investigation. The research of the mechanical properties of the bearing, when it is under tensile deformation, is rather limited. Under extreme displacements of the bearings, there might be important degradation of the stiffness, both compressive and tensile of the bearings.

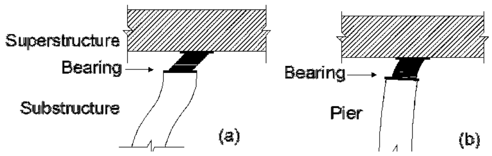

Fig. 1 - Current codes of practice showing isolated deflected bridge pier-(a) AASHTO [21] and (b) EN 1998-8 [24]

The behaviour of steel-laminated elastomeric bearings under dynamic loading (cyclic shear displacements) in combination with variable axial loads, for extreme seismic displacements, is investigated in this paper. Such types of bearings are used extensively in multi-span simply supported pre-stressed concrete bridges with I-beams. Validation of the numerical models of this study was based on recently published literature [13]. Another issue, that is investigated, is the development of local tensile stresses within the elastomer for different boundary conditions of the isolator, given that the deflection of the pier and the rotation of the deck impose relative movements and rotations to the bearings. The mechanical properties that are used for the design of the model are the properties of the hyperelastic Ogden model [25].

2. Validation of the steel-laminated elastomeric bearing

2.1 Use of steel-laminated elastomeric bearings in multi-span simply supported bridges

A multi-span simply supported bridge, like the one shown in Fig. 2, makes use of elastomeric bearings like the one modelled and analysed in this paper. The numerical models and the loading on the bearings, analysed in this paper, are simplified loading patterns identified on the bridge of Fig. 2. This is a typical bridge which is used extensively in southern Europe. There are simply supported pre-stressed concrete I-beams which are seated on two lines of five elastomeric bearings on each pier and one line of bearings at the abutments.

The total length of these bridges depends on the number of the spans and span length, which typically varies between 20 m and 35 m. Each span consists of in-situ concrete slab, of a transverse width of 13.45 m, where ordinary reinforcement and five pre-cast I-beams are used. Two lines of five elastomeric bearings are located at the top of the piers for the support of the I-beams. Hence, there is a total of ten steel-laminated elastomeric bearings on each pier and five on each abutment. The total depth of the deck is comprised of the depth of the slab which is 0.25 m thick and of the depth of the pre-cast concrete beams that is 1.75 m. The piers of the bridge are circular with diameter of 2.50 m and their height varies from H= 10 m up to H= 30 m. The foundation is comprised of 3 by 3 piles groups.

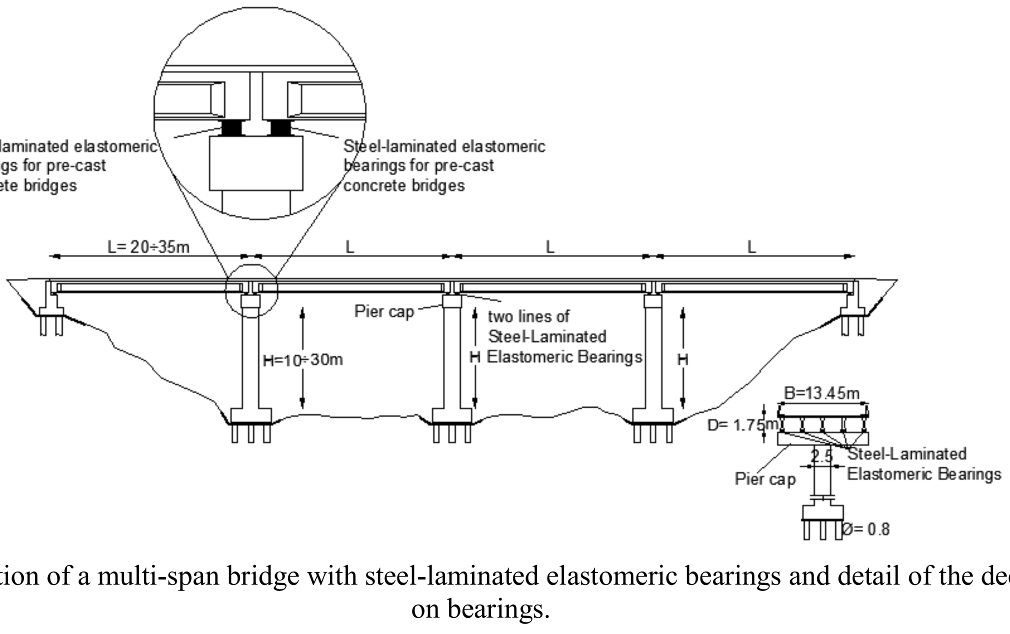

Fig. 2 – Elevation of a multi-span bridge with steel-laminated elastomeric bearings and detail of the deck support on bearings.

2.2 Numerical model of steel-laminated elastomeric bearing

The geometry of the benchmark bearing is given in Fig. 3 and Table 1. This is a circular bearing with diameter of 700 mm. Circular anchor plates with a diameter of 1000 mm are used at the top and bottom of the bearing. The bearing is comprised of two anchor plates with a total of 30 layers of elastomer alternating with 29 steel shims. The 30 layers of elastomer have 4 mm thickness each, hence a total thickness of the elastomer of 120 mm is reached. The thickness of each one of the 29 steel shims is 3.1 mm with the total thickness of the steel shims being 89.9 mm. The two top and bottom anchor plates have a thickness of 28 mm each. Therefore, the total thickness of the benchmark bearing is 265.9 mm (Ø700 x 265.9 (4)). The diameter of the elastomeric layers and steel shims is 700 mm, the diameter of the anchor plates is 1000 mm and at the centre of the bearing there is a hole with 15 mm diameter.

The Ogden hyperelastic material [25] model was used for the modelling of the elastomeric layers of the benchmark bearing, which represents Low Damping natural Rubber Bearings (LDRB). According to Eurocode 8 – Part 2 [24] LDRBs have a damping ratio $\xi < 6\%$.The stresses that are developed within the elastomer, as well as the energy dissipation (hysteresis) within the bearing are described accurately by the hyperelastic Ogden material. The Eq. (1) defines the Ogden strain energy density function:

$$U = \sum_{n=1}^{2} \frac{\mu_n}{\alpha_n}\left(\bar{\lambda}_1^{\alpha_n} + \bar{\lambda}_2^{\alpha_n} + \bar{\lambda}_3^{\alpha_n} - 3\right) + 4.5B\left(J^{\beta} - 1\right)^2 \quad (1)$$

The hyperelastic parameters from Eq. (1) are μ_1= 0.41 MPa, α_1= 1.6, μ_2= 0.0012 MPa, α_2= 6.2 and β=1/3. These values were obtained from experiments of a rubber bearing with variable pressure levels, similar to a recent literature [26]. J is the elastic volume ratio and $\bar{\lambda}_1$, $\bar{\lambda}_2$, $\bar{\lambda}_3$ are the deviatoric stretches, i.e. the principal values of right stretch tensor. The shear modulus and the Poisson ratio are calculated as per the reference case and are described by Eq. (2) and Eq. (3), where B is the bulk modulus and is equal to 1000 MPa:

$$G_b = \alpha_1\mu_1 + \alpha_2\mu_2 \Rightarrow G_b = 0.66344 \text{ MPa} \quad (2)$$

$$\nu = \left(\frac{3B}{G_b} - 2\right) / \left(\frac{6B}{G_b} - 2\right) \Rightarrow \nu = 0.49989 \quad (3)$$

The FEA software program ABAQUS ver. 6.13 was used to perform all numerical simulations and analyses as the software can take into account large geometric non-linearities.

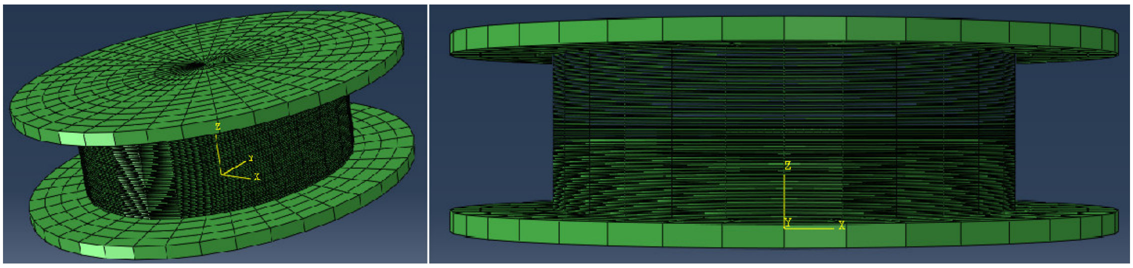

Fig. 3 – Meshing of the benchmark bearing: 3D model and side view

Table 1 – Geometrical characteristics of the benchmark bearing

	notation (unit)	value
diameter of the elastomer	D_r (mm)	700
diameter of the anchor plate	D_{AP} (mm)	1000
diameter of the hole	D_h (mm)	15
area of the elastomer layer	A_b (mm^2)	384845

	notation (unit)	value
total height of the bearing	T (mm)	265.9
elastomer layer thickness	t_r(mm)	4
number of elastomeric layers	n_r	30
total elastomer thickness	T_r (mm)	120
single steel shim thickness	t_s(mm)	3.1
number of steel shims	n_s	29
total steel shim thickness	T_s(mm)	89.9
single anchor plate thickness	t_{AP}(mm)	28
number of anchor plates	n_{AP}	2
total anchor plate thickness	T_{AP} (mm)	56

2.3 Validation of the benchmark bearing

The validation of the benchmark bearing against existing recent literature [13] can be seen in Fig. 4. The bottom anchor plate, of the bearing, is fixed. Shear displacement of 450 mm (i.e. shear strain of 375%) with simultaneous axial pressure of 14 MPa are imposed to the bearing. One full cycle of loading unloading in shear, corresponding to a shear strain of 375%, was imposed to the bearing. The comparison, between the results of the analysis with the benchmark bearing and the available results of the existing recent literature [13], is shown in Fig. 4. It can be observed that the reproduction of the force-deformation diagram of the available numerical (red line) and experimental (dashed lines) results of previous studies [13] with the benchmark bearing (black line) is accurate. The analyses that will be presented in the following sections of this paper were conducted with the benchmark bearing described above.

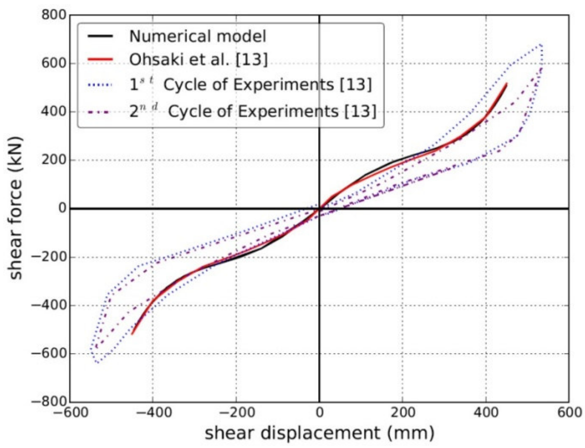

Fig. 4 - Validation of the benchmark bearing

3. Response of the elastomeric bearing and development of local tensile stresses

3.1 Parametric study

In this paper, the properties and response of steel-laminated elastomeric bearings were defined. In particular, the stiffness and dissipation capacity, as well as local effects e.g. concentration of local tensile stresses are examined. The loading conditions that are applied to the benchmark bearing are: shear strain of 375% combined with variable axial loads, compressive or tensile, ranging from 2 MPa to -14 MPa with the intermediate values being 0 MPa, -2 MPa, -5 MPa and -10 MPa. For the parametric study, the bottom anchor plate of the model is fixed, while the upper anchor plate of it is free to rotate. Large shear strain values were applied to the isolator, given that, such loads are observed in large-scale structures like bridges. Also, bearings experience tension and extreme shear strains above the codes provisions [10].

When the isolators are subjected to large shear displacements they exhibit instabilities such as buckling. Therefore, in order to understand the response of the isolators, under such conditions, this value of shear strain (375%) was chosen. Additionally, the response of the isolators when they are subjected to tensile loading was also studied. A shear displacement of 375% simultaneously with a maximum axial tensile load of 2 MPa was applied to the bearing to study in detail the response of the isolators used in the bridge shown in Fig. 2.

Two full cycles of loading-unloading at ±375% shear strain were imposed to the isolator. In order for the hysteresis loops from the analyses to be obtained and to capture the damping properties of the bearing, the hysteretic parameters of ABAQUS were used. The values of the hysteretic parameters derived from the paper of Bergström & Boyce [27].

Regarding the response of the isolator when the shear strain is 375%, Table 2 summarises the obtained results. It can be observed, in Table 2, that the stiffness of the isolator is decreased while the imposed axial load is increased. For example, when the imposed compression is increased from 5 MPa to 10 MPa, then there is a decrease of 14.12% of the stiffness of the isolator. The corresponding percentage of decrease when 14 MPa axial pressure is imposed, in comparison to 10 MPa axial pressure, to the isolator is almost the same, i.e. 13.94%. Regarding the influence of the second cycle of loading-unloading, on the stiffness of the isolator, the results in Table 2 show that there is negligible increase of the stiffness of the isolator from the first to the second cycle of loading-unloading. For example, when the compressive load is 2 MPa, then there is 1.31% increase from the first to the second cycle of loading-unloading, which is negligible. The corresponding percentage of increase, from the first to the second cycle of loading, when the compressive load is 5 MPa, is 2.43%.

Regarding the damping ratio of the isolator, it is observed that, there is increase of the damping ratio when the axial load is increased. When there is increase of the axial compressive load from 0 MPa to 2 MPa, there is negligible increase of the damping ration of the percentage of 4.7%. Additionally, when the compressive load increases from 2 MPa to 5 MPa, there is 6.15% increase of the damping ratio. From 5 MPa to 10 MPa the increase of the damping ratio is 23.55% and when the compressive load increases from 10 MPa to 14 MPa the percentage of increase of the damping ratio is 20%. Regarding the second cycle of loading-unloading, the damping ratio of the isolator is decreased in all cases. The maximum decrease of the damping ratio, from the first to the second cycle of loading-unloading, is observed when there is tension of 14 MPa and the percentage of decrease is 10.68%.

It is observed in Fig. 5 that, when the shear strain remains the same and the axial pressure that is imposed to the isolator is increased, then the value of the stiffness that is developed at the isolator is decreased. The former observation is in line with previous studies [8]. Nonetheless, the aforementioned finding was found to be the case when the target displacements are larger than 200 mm, i.e. shear strains larger than 167%. In the cases where the shear strains are smaller, the stiffness was found to be initially increased, then decreased and then increased again for larger shear strains when the vertical compression is 14 MPa, whilst the behaviour of the bearing was found to be almost linear when the compression is relatively low, i.e. up to 2 MPa. Based on the hysteresis loops shown in Fig. 5 the damping ratio ξ is calculated based on Eq. (4):

$$\xi = \frac{A}{2*\pi*K_{eff}*D^2} \tag{4}$$

A is the area of the hysteresis loop which is extracted from Fig. 5, K_{eff} is the effective stiffness of the bearing measured at the maximum target displacement of 450 mm and D is the displacement amplitude.

Table 2– Influence of the axial compressive load to the response of the isolator (stiffness and damping ratio)

	tension 2MPa		**unloaded 0 MPa**		**compression 2MPa**		**compression 5MPa**		**compression 10MPa**		**compression 14MPa**	
Cycles	**1st**	**2nd**	**1st**	**2nd**	**1st**	**2nd**	**1st**	**2nd**	**1st**	**2nd**	**1st**	**2nd**
K_{eff} (kN/m)	2327	2361	2318	2349	2207	2236	2096	2147	1800	1829	1549	1569
ξ_{hyst}	2.15%	1.98%	2.33%	2.32%	2.44%	2.41%	2.59%	2.34%	3.2%	2.93%	3.84%	3.43%

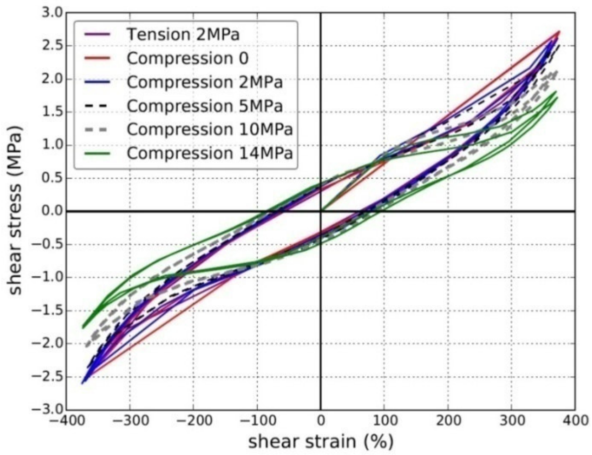

Fig. 5 - Response of the benchmark bearing under variable axial loads (shear strain375%)

3.2 Influence of the boundary conditions on the response of the isolator

The analysis for shear strain of 375% and compression of 10 MPa was repeated for two different boundary conditions: (a) the bearing is fixed at the bottom anchor plate but free to rotate at the top and (b) the bottom anchor plate is fixed, i.e. $UX=UY=UZ=RX=RY=RZ=0$, and the top anchor plate is restricted to rotate and remains parallel to the bottom one, i.e. $RX=RY=RZ=0$ and it is free to move along X, Y and Z axes i.e. $UX\neq0$, $UY\neq0$, $UZ\neq0$. The aforementioned boundary conditions were chosen for this study, given that they reflect the two cases that met in practical designs, i.e. when the bearing exhibits rotations, thus allow for relative rotations of the upper and the lower anchor plates or the isolator exhibits negligible rotations, thus the upper anchor plate displaces almost parallel to the bottom one. It is important to keep the rotation of the isolator within allowable limits [3].

The isolation bearings on buildings have a predominantly translational movement, whilst rotations are negligible. On the other hand, bearings that are used on piers in order for the bridge decks to be supported might exhibit significant rotations due to the deflection of the piers and the rocking of the foundation [28]. The hysteresis loop of the bearing, when it is subjected to shear strain of 375% and axial compressive stress of 10 MPa, is depicted in Fig. 6. It illustrates the bearing responses for different boundary conditions of it, i.e. when the top anchor plate is free to rotate or its rotations are restricted. Table 3 shows the values of the shear stiffness and damping ratio for the two analyses that were performed with different boundary conditions.

Table 3– Influence of the boundary conditions to the response of the isolator (stiffness and damping ratio) – shear strain 375% and compressive load 10 MPa

	upper anchor plate free to rotate	**restraint of the rotation of the upper anchor plate**
K_{eff} (kN/m)	1800	2113
ξ_{hyst}	3.2%	2.05%

As it is shown in Table 3 when there is restraint rotation the stiffness of the isolator is increased by 17.39% and the damping ratio is decreased by 35.94%. The design of bridge abutments, piers and foundations is based on the period of the isolated structure and hence, the stiffness of the isolator is of great importance to the design of structures subjected to static or dynamic loads. On the other hand, the forces transmitted from the bearings to the substructures are the ones used for designing the reinforcements and the size of foundations. Additionally, the design of the expansion joints is dependent on the displacements of the deck and thus the stiffness of the isolation system. It is observed from Table 3 and Fig. 6 that there is significant influence, both to the stiffness and the damping of the isolator, from the boundary conditions that are implemented to the bearing. The stiffness of the isolator is increased when there is additional restraint, whilst on the other hand the damping of the isolator is decreased.

Additionally, Fig. 6 shows that the response of the isolator is essentially linear, for a maximum shear strain of 375%, when the rotation of the upper anchor plate is restrained and the imposed shear strain is larger than 100%. Contrarily, the behaviour of the isolator when the upper anchor plate is free to rotate had already been studied at the results of shear tests [1]. In the latter case, the bearing stiffness decreases after the displacement of 240 mm, i.e. after a shear strain of 200% is applied, whilst its stiffness increases again at higher shear strains, i.e. 250% that corresponds to shear displacement of 300 mm.

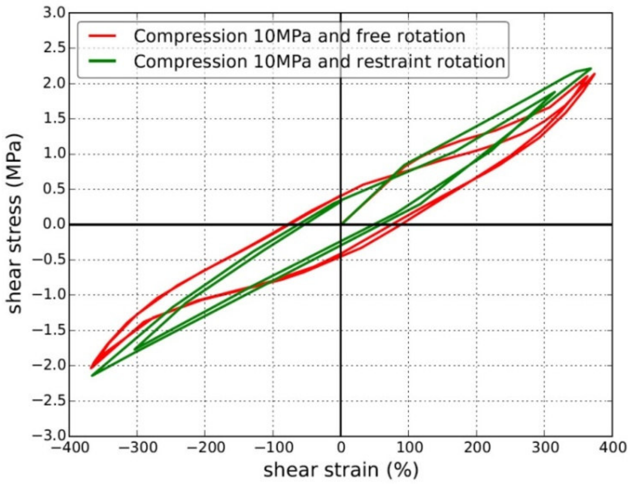

Fig. 6 - Response of the benchmark bearing for different boundary conditions (shear strain 375% - compression 10 MPa)

3.3 Influence of the boundary conditions on the development of local tensile stresses

In order to identify the development of tensile stresses shown in Fig. 7, 8 and 10 as S33, shear strains of 375% together with 10 MPa axial compression and two different boundary conditions were analysed: (a) upper anchor plate free to rotate as shown in Fig. 7 and (b) restraint rotation of the upper anchor plate as per Fig. 8. Fig. 7 and 8 show vertical cuts, at the position where 375% shear strain was imposed to the isolator during the first cycle of loading-unloading, along the diameter of the reference circular bearing with the same axial compressive load of

10 MPa and boundary conditions as described. It is noted that the values of the numerically calculated stresses within the elastomeric bearings did not consider the potential of local cavitation and hence the stresses are hypothetical in the sense that the elastomer remains elastic.

It is observed that when the upper anchor plate is free to rotate, then the bearing is rotated by 4.66 degrees. The grey areas that are shown in Fig. 7 and 8 are areas where local tensile stresses are developed. It is observed that when there is restraint of the rotation of the upper anchor plate then the values of the local tensile stresses that are developed within the isolator are significantly smaller. The latter explains the rotation limits proposed in design guidelines of steel laminated rubber bearings.

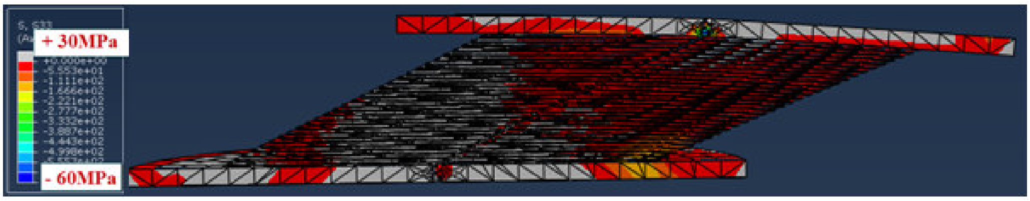

Fig. 7 - Vertical section for upper layer of the benchmark bearing free to rotate – hypothetically the elastomer remains elastic

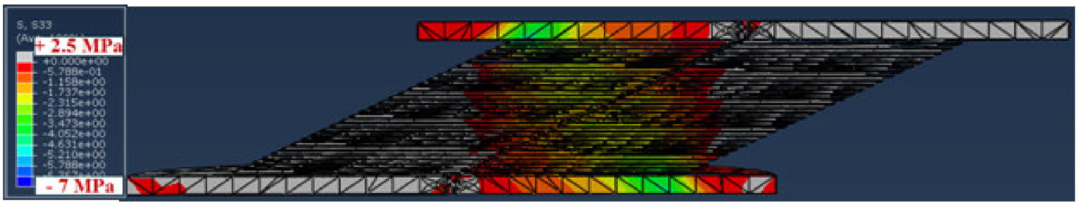

Fig. 8 - Vertical section for application of rotational restraint to the upper layer of the benchmark bearing

Fig. 9 shows the steel shim and elastomeric layer which were monitored to assess the development of local tensile stresses. Fig. 10 a, b, c and d illustrate the horizontal sections of the middle steel shim and the middle elastomeric layer, at the position where 375% shear strain was imposed to the isolator during the first cycle of loading-unloading, when the upper layer is free to rotate (Fig.10a and 10b) and when a rotational restraint is applied on the upper anchor plate of the bearing (Fig. 10c and 10d). Emphasis is given to the development of local tensile stresses (grey colour). In the case that rotation of the upper layer is allowed, there is development of local tensile stresses only at the one edge of the isolator (Fig. 10a and 10b, left hand side in Fig. 7).

The numerical results also showed that, the rotational restraint of the upper anchor plate of the elastomeric bearing reduces drastically the tensile stresses that are developed towards the centre of the bearing. Based on Fig. 10c, tensile stresses of the value of 1.43 MPa are developed at the edges of the steel shim, whilst the tensile stresses that are developed at the edges of the elastomeric layer are approximately 1.62 MPa. Thus, the magnitude and the distribution of the tensile stresses within the elastomeric bearing are influenced strongly by the bearing boundary conditions. The analyses revealed that the boundary conditions that were imposed to the bearing were important with regard to the developed tensile stresses within the elastomer

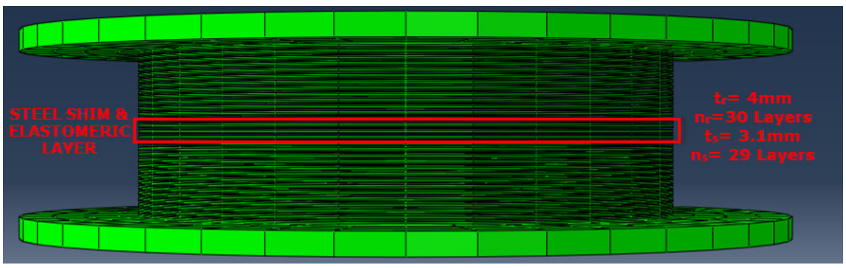

Fig. 9 – Indication of the position of the steel shim and elastomeric layer which are used at the following figures

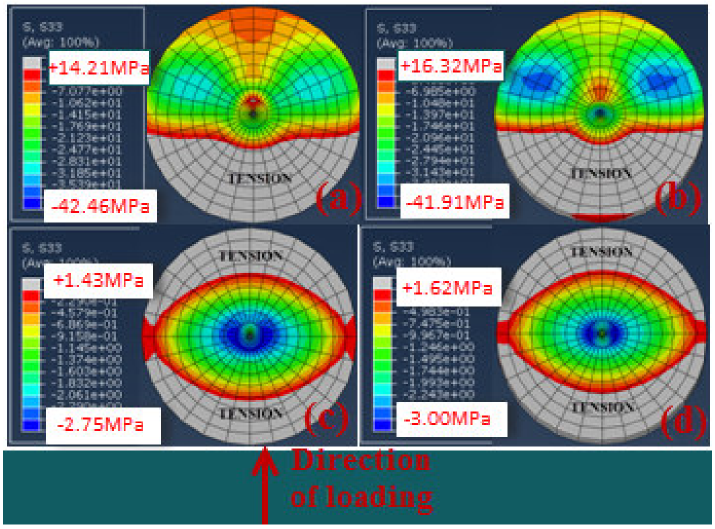

Fig. 10 - Axial stresses within the bearings for 375% shear strain at: (a) middle steel shim and (b) middle elastomeric layer when the upper layer is free to rotate, and horizontal section of the (c) middle steel shim and (d) middle elastomeric layer when there is restraint of the rotation of the upper layer

4. Conclusions

The use of steel-laminated elastomeric bearings, as seismic isolation devices (amongst others, such as viscous dampers and Shock Transmitted Units), for typically pre-stressed concrete bridges and their behaviour under large cyclic shear displacements combined with variable tensile and compressive axial loads and boundary conditions are presented in this paper. Experimental validation of this study would benefit the outcome of the research.

The following conclusions may be obtained:

- There is significant reduction, of the value of 13.94%, in the shear stiffness of the isolator and at the same time the dissipation capacity of the isolator is increased, with 20%, when the compressive load on the bearing increases from 10 MPa to 14 MPa.
- An increase in the shear stiffness combined with a decrease in the damping ratio, with percentages of 17.39% and 35.94% respectively, was observed when the boundary conditions of the upper anchor plate of the bearings changed from free rotation to restrained rotation, with shear strain of 375% and compressive axial load of 10 MPa.
- Despite the fact that only shearing and axial compression were imposed to the bearing (shear strain of 375% and compressive load of 10 MPa), at the case where the bearing is allowed to rotate freely, tensile stresses exceeding 2 MPa were found to be developed within the elastomer. On the other hand, there is development of local tensile stresses smaller than 2 MPa when there is rotational restraint of the upper anchor plate. Thus the design of elastomeric bearings should ensure that both the pier top and the deck do not exhibit significant rotations under earthquake excitations.
- Based on the numerical analyses, the number of loading-unloading cycles influences the behaviour of the isolators. The stiffness of the isolator is increased after the first cycle, while the dissipation capacity is decreased. More specifically, when the compressive load that was applied to the isolator was 5 MPa, the stiffness of the isolator increase from the first to the second cycle with 2.43% while the damping ratio decreased by 9.65%. However, this finding did not take into account the potential softening of the isolator which may be occur due to the large tensile stresses that are developed within the elastomer under large shear strains.

5. References

[1] Tubaldi E, Mitoulis AS, Ahmadi H, Muhr A, (2016): A parametric study on the axial behaviour of elastomeric isolators in multi-span bridges subjected to horizontal excitations. *Bulletin of Earthquake Engineering,* **14** , 1285-1310.

[2] Aria M, Akbari R, (2013): Inspection, Condition Evaluation and Replacement of Elastomeric Bearings in Road Bridges. *Structure and Infrastructure Engineering,* **9** (9), 918-934.
[3] Stanton JF, Roeder CW, Mackenzie-Helnwein P., White C., Kuester C., Craig B., (2008): *Rotation Limits for Elastomeric Bearings*. National Cooperative Highway Research Program (NCHRP), Washington D.C.: Transportation Research Board.
[4] Chen WF, Duan L (2003): *Bridge Engineering: Seismic Design (Principles and Applications in Engineering)*. CRC Press, Boca Raton
[5] Nguyen HH, Tassoulas JL, (2010): Directional Effects of Shear Combined with Compression on Bridge Elastomeric Bearings. *Journal of Bridge Engineering,* **15** (1), 73-80.
[6] Mitoulis SA, (2014): Uplift of Elastomeric Bearings in Isolated Bridges Subjected to Longitudinal Seismic Excitations. *Structure and Infrastructure Engineering,* 1-16.
[7] Kelly JM, Konstantinidis D, (2011): Mechanics of rubber bearings for seismic and vibration isolation. *John Wiley & Sons*.
[8] Manos GC, Mitoulis S, Kourtidis V, Sextos V, Tegos I, (2007): Study of the Behaviour of Steel Laminated Rubber Bearings under Prescribed Loads. *10th World Conference on Seismic Isolation, Energy Dissipation and Active Vibrations, Control of Structures,* Istanbul, Turkey.
[9] Kumar M, Whittaker AS, Constantinou MC, (2014): An Advanced Numerical Model of Elastomeric Seismic Isolation Bearings. *Earthquake Engineering & Structural Dynamics,* **43** , 1955-1974.
[10] Kumar M, Whittaker AS, Constantinou MC, (2015): Response of Base-Isolated Nuclear Structures to Extreme Earthquake Shaking. *Nuclear Engineering and Design*, **295** , 860–874.
[11] Mitoulis S, Muhr A, Ahmadi H, (2014): Uplift of Elastomeric Bearings in Isolated Bridges- A Possible Mechanism: Effects and Remediation. *2nd European Conference on Earthquake Engineering and Seismology,* Istanbul, Turkey.
[12] Constantinou MC, Whittaker AS, Kalpakidis Y, Fenz DM, Warn GP, (2007): Performance of Seismic Isolation Hardware under Service and Seismic Loading. *Multidisciplinary Center for Earthquake Engineering Research (MCEER),* New York: University at Buffalo.
[13] Ohsaki M, Miyamura T, Kohiyama M, Yamashita T, Yamamoto M, Nakamura N, (2015): Finite-Element Analysis of Laminated Rubber Bearing of Building Frame under Seismic Excitation. *Earthquake Engineering & Structural Dynamics,* **44** (11), 1881-1898.
[14] Gent AN, Lindley PB, (1958): Internal Rupture of Bonded Rubber Cylinders in Tension. *Proceedings of the Royal Society of London. Series A, Mathematical, Physical and Engineering Sciences*, **249** (1257), 195–205.
[15] Kwon OS, Jeong SH, (2013): Seismic Displacement Demands on Skewed Bridge Decks Supported on Elastomeric Bearings. *Journal of Earthquake Engineering*, **17** (7), 998-1022.
[16] Takahashi Y, (2012). Damage of Rubber Bearings and Dampers of Bridges in 2011 Great East Japan Earthquake. *Proceedings of the International Symposium on Engineering Lessons Learned from the 2011 Great East Japan Earthquake*, Tokyo, Japan.
[17] Kawashima K, Matsuzaki H, (2012). Damage of Road Bridges by 2011 Great East Japan (Tohoku) Earthquake. *15th World Conference of Earthquake Engineering*, Lisbon, Portugal.
[18] Kawashima K, Kosa K, Takahashi Y, Akiyama M, Nishioka T, Watanabe G, Koga H, Matsuzaki H, (2011). Damages of Bridges during 2011 Great East Japan Earthquake. *Proceedings of 43rd Joint Meeting, US-Japan Panel on Wind and Seismic Effects,* Tsukuba Science City, Japan.
[19] EN 1337-3: 2005, (2005): *Structural bearings – Part 3: Elastomeric Bearings*. Brussels: European Committee for Standardization.
[20] BS EN 15129: 2009, (2010): *Anti-seismic Devices.*BSI British Standards.
[21] American Association of State Highway and Transportation Officials, AASHTO, (2014): *Guide Specifications for Seismic Isolation Design.* 4th Ed. Washington, DC.
[22] Japan Road Association, JRA, (2011): *Bearing Support Design for Highway Bridges.* Tokyo, Japan.
[23] Yang RQ, Liu WG, He WF, Feng DM, (2010): Tensile Stiffness and Deformation Model of Rubber Isolators in Tension and Tension-Shear States. *Journal of Engineering Mechanics*, **136** (4), 429-437.

[24] EN 1998-2, (2005): *Eurocode 8: Design of Structures for Earthquake Resistance, Part 2: Bridges*. Brussels, Belgium: European Committee for Standardization.
[25] Ogden WR, (1972): Large Deformation Isotropic Elasticity–On the Correlation of Theory and Experiment for Incompressible Rubber like Solids. *Proceedings of the Royal Society of London. Series A, Mathematical and Physical Sciences*, **326** (1567), 565–584.
[26] Bradley LG, Chang CP, Mckenna BG, (2001): Rubber Modelling Using Uniaxial Test Data. *Journal of Applied Polymer Science*, **81**^{0}, 837-848.
[27] Bergström JS, Boyce MC, (1998): Constitutive Modelling of the Large Strain Time-Dependent Behaviour of Elastomers. *Journal of Mechanics Physics Solids*, **46**^{0}, 931-954.
[28] Mitoulis SA, (2007): Bridges with Fixities and Bearings VS Isolated Systems. *COMPDYN 4th International Conference in Computational Methods in Structural Dynamics and Earthquake Engineering*, 12-14 June 2013, Kos, Greece.